Journal of Radioanalytical and Nuclear Chemistry (2018) 316:331–339
https://doi.org/10.1007/s10967-018-5736-1

Synthesis and adsorption characteristics of calix[6]arene derivative modified *Aspergillus niger*-Fe_3O_4 bio-nanocomposite for U(VI)

Le Li[1,2] · Shuangyang Tang[3] · Bin Cheng[1,2] · Qi Liao[2] · Wei Lu[1,2] · Zhongran Dai[2] · Yan Tan[1,2] · Jing Sun[2]

Received: 21 December 2017 / Published online: 17 February 2018

Abstract
A new type of magnetic bioadsorbent (CDAB) was synthesized by reaction of amidoxime modified calix[6]arene derivative with the *Aspergillus niger*-Fe_3O_4 bio-nanocomposite, the bioadsorbent have been well characterized with FT-IR, SEM-EDS, XPS and VSM. The effects of various experimental parameters include pH, contact time, initial uranium(VI) concentration, adsorbent dosage and temperature on the bioadsorption of uranium(VI) were investigated in detail. Adsorption experimental results showed the adsorption process of CDAB was pseudo-second order kinetic model and Langmuir adsorption isotherm model. The maximum adsorption capacities of CDAB were calculated to be 77.04 mg g^{-1} for uranium(VI). The adsorption efficiency of CDAB towards U(VI) could reach at 83.6% with a considerable selectivity. In addition, the thermodynamic parameters indicated that the adsorption process was spontaneous and endothermic.

Keywords Uranium(VI) · *Aspergillus niger*-Fe_3O_4 bio-nanocomposite · Calix[6]arene · Magnetic bioadsorbent

Introduction

Uranium is the main source of nuclear fuel and has been widely used in the nuclear industry. However, large amount of uranium-containing wastewater poses a serious threat to the organism and environment due to the radioactive and toxic of uranium [1, 2]. Therefore, developing effective techniques for the segregation of uranium(VI) from uranium-containing wastewater is an important issue for the environmental remediation.

In the past decades, many methods for removal of uranium(VI) from low concentration uranium waster waste have been proposed, such as liquid–liquid extraction, chemical precipitation, evaporation concentration, ion exchange and adsorption [3–6]. As a potential low-concentration uranium wastewater treatment method, a lot of adsorbents have been developed to adsorb uranium(VI) from uranium-containing wastewaters, such as carbon nanotubes, graphene oxides, magnetic materials, biomass and so on [7–17]. However, there are a number of drawbacks among this adsorbents, such as low adsorption capacity and selectivity, slow kinetics and poor water/chemical stability. Thus, it is still a need to develop new adsorbent materials for efficient adsorb uranium(VI) from uranium-containing wastewaters.

Biological adsorbents have got a wide range of applications due to the advantages of low cost, effective mass transfer and no secondary pollution. In addition, magnetic nanoparticles have attracted considerable attention due to their magnetic properties and nanoscale features. Therefore, the magnetic biosorbent as high performance adsorbents for the removal of uranium(VI) have attracted considerable attention. For example, Han et al. [18] reported a fungus-Fe_3O_4 bio-nanocomposite which showed the saturated sorption capacity up to 171 mg g^{-1} for uranium(VI) within only 4 h; Wang et al. [19] reported a novel fungus-Fe_3O_4 bio-nanocomposite which exhibited

✉ Le Li
usclile@126.com

[1] School of Public Health, University of South China, Hengyang 421001, People's Republic of China

[2] Hunan Province Key Laboratory of Green Development Technology for Extremely Low Grade Uranium Resources, University of South China, Hengyang 421001, People's Republic of China

[3] Institute of Pathogenic Biology, University of South China, Hengyang 421001, People's Republic of China

excellent regeneration performance for the pre-concentration of radionuclides.

Recently, calixarene derivatives are also used for adsorption of uranium(VI) because of their simple preparations, easy modifications, low toxicity, and unique extraction properties of metal ions. For example, Zhang et al. [20] reported an amidoxime group modified calix[8]arene (C8A-AO) which exhibited excellent selective adsorption capacity for the uranium(VI).

Based on the above mentioned advantages of magnetic biosorbent and calixarene derivative, in this work, we synthesized a novel magnetic bioadsorbent (CDAB) by reaction of amidoxime modified calix[6]arene derivative with the *Aspergillus niger*-Fe_3O_4 bio-nanocomposite (ANBN). The calix[6]arene derivative modified *Aspergillus niger*-Fe_3O_4 bio-nanocomposite was characterized by FT-IR, SEM-EDS, XPS and VSM, and the adsorption behavior of uranium(VI) was also investigated in detail. The results show that the CDAB is expected to have potential application for the adsorption of uranium(VI) from aqueous solutions.

Experimental

Characterizations

Fourier-transform infrared (FT-IR) spectra of the samples were measured by IR Prestige-21 using standard KBr pellets. The morphology of synthetic products was characterized using scanning electron microscope (SEM, Zeiss Merlin microscope). The MPMS SQUID VSM (vibrating sample magnetometer) was applied to test magnetic properties through measuring the function between magnetization and applied-field from − 10 to 10 kOe at 300 K. X-ray photoelectron spectroscopy (XPS) of samples was measured by ESCALAB 250Xi.

Preparation of HHHC-AN

NaH (0.3 g) and 37,38,39,40,41,42-Hexahydroxyl-1,8,13,19,25,31-hexacarboxy calix[6]arene (HHHC, 0.9 g) were stirred at room temperature in DMF (40 mL). Bromoacetonitrile (1.1 g) was added, and the mixture was stirred at 75 °C for 24 h. H_2O (80 mL) was added, and the suspension was cooled to room temperature and filtrated. The residue solid was taken up in CH_2Cl_2 (100 mL); washed with 1 N HCl (2 × 50 mL), saturated NH_4Cl (3 × 50 mL), and brine (50 mL); and dried with $MgSO_4$. After filtration, CH_2Cl_2 was evaporated, and the residue was treated with methanol yielding a pure white solid.

Preparation of HHHC-AO

200 mg HHHC-AN and 1 mL NH_2OH were dispersed into 40 mL methanol–water ($V_m/V_w = 1/1$) solution. The mixed suspension was kept being stirred at 80 °C for 12 h. After cooling to room temperature, the solid was isolated by applying external magnetic field and washed with ethanol and deionized water for several times. The product was kept being dried in vacuum at 50 °C for 24 h.

Preparation of CDAB

HHHC-AO (1.0 g) stirred at room temperature in $CHCl_3$ (50 mL), $SOCl_2$ (5.0 mL) was dropwise added. The mixture was heated to reflux for 4 h. The suspension was cooled to room temperature. $CHCl_3$ and $SOCl_2$ was evaporated to obtain the intermediate product, then a solution of the intermediate product (1 g) and trimethylamine (2 mL) in 20 mL of $CHCl_3$ was added to a solution of ANBN (1 g) in 40 mL of DMF/H_2O (DMF/H_2O = 4:1). The mixture was stirred at 75 °C overnight, then cooled to room temperature, and evaporated under reduced pressure. The product was washed with $CHCl_3$ and H_2O. Finally, the obtained product was dried in a vacuum at 60 °C for 24 h.

Adsorption experimental

The effects of pH, contact time, initial uranium concentrations, coexisting ions and temperature on the U(VI) adsorption by CDAB were investigated in detail. Typically, 30 mg adsorbent was added to a U(VI) solution (100 mL) with appropriate concentration and appropriate pH value in a 250 mL beakerflask shaken in air bath oscillator at 180 rpm and appropriate temperature. The pH was adjusted by a negligible volume of dilute HNO_3 or NaOH. After the beaker flask was shaken for predetermined time, the solid–liquid separation was conducted using a magnet. The concentration of U(VI) in the solution was analyzed by the Br-PADAP method with a Visible Spectrophotometer at 578 nm (National Standard of the People's Republic of China, EJ 267.4-1984). All the experiments were performed in duplicates and a blank sample was set at the same time to minimize experimental error.

The removal efficiency [E (%)], amount of U(VI) adsorbed on the adsorbent (q_e) and distribution coefficient K_d (mL/g) were calculated using the following formulas:

$$E(\%) = \frac{(C_o - C_e)}{C_o} \times 100, \quad (1)$$

$$q_e = \frac{(C_o - C_e)V}{m}, \quad (2)$$

$$K_d = \frac{C_o - C_e}{C_e} \times \frac{1000\ V}{m}, \quad (3)$$

where q_e is the equilibrium adsorption capacity (mg/g), C_o and C_e are the concentrations of U(VI) before and after adsorption (mg/L), respectively, V is the liquid phase volume (L), and m is the amount of adsorbent (g).

Results and discussion

Characterization of materials

The calix[6]arene derivative modified *Aspergillus niger*-Fe_3O_4 bio-nanocomposite (CDAB) was synthesized according to the Scheme 1. HHHC and ANBN were synthesized according to the reported procedures [19, 21]. Figure 1 shows the FT-IR spectra of HHHC, HHHC-AN and HHHC-AO. After modifying the nitrile group on the HHHC, the peak of –OH at 3227 cm^{-1} was disappear in the spectrum of HHHC-AN, and a new characteristic peak of C≡N at 2240 cm^{-1} was observed in the spectrum of HHHC-AO. After hydroxylamine treatment, the peak at 2240 cm^{-1} disappear and the new characteristic peaks for $–NH_2$ (or –OH), C=N and N–O appear at 3188, 1666 and 918 cm^{-1}, respectively, which indicated that the nitrile groups in HHHC-AN were completely converted into the amidoxime group. As shown in Fig. 2, for CDAB, the peaks of 3373, 2927, 1659 and 625 cm^{-1} were related to the amino (or hydroxyl), benzene ring, C=N and Fe–O, respectively, which indicated that the CDAB bioadsorbent was successfully prepared.

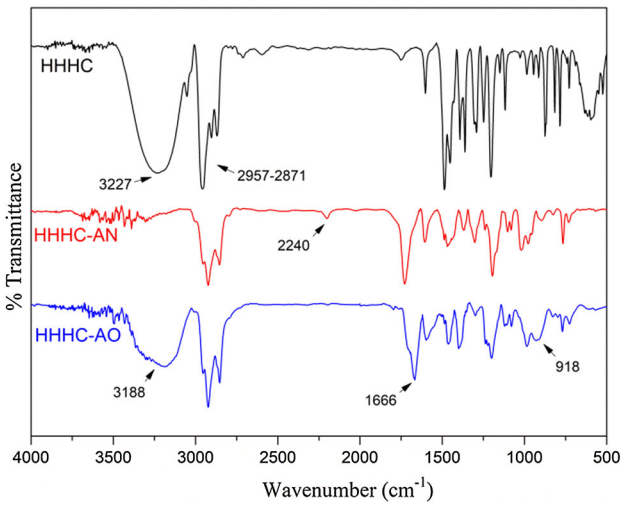

Fig. 1 FT-IR spectra of HHHC, HHHC-AN and HHHC-AO

The microstructure of ANBN and CDAB were studied by SEM. The SEM images of ANBN and CDAB were shown in Fig. 3. Obviously, the surface of CDAB became rougher and uneven, which was related to the modification by calix[6]arene derivative (HHHC-AO).

The magnetization curves of ANBN and CDAB were shown in Fig. 4. It was clearly seen that the saturation magnetization of ANBN (6.63 emu/g) more highly than

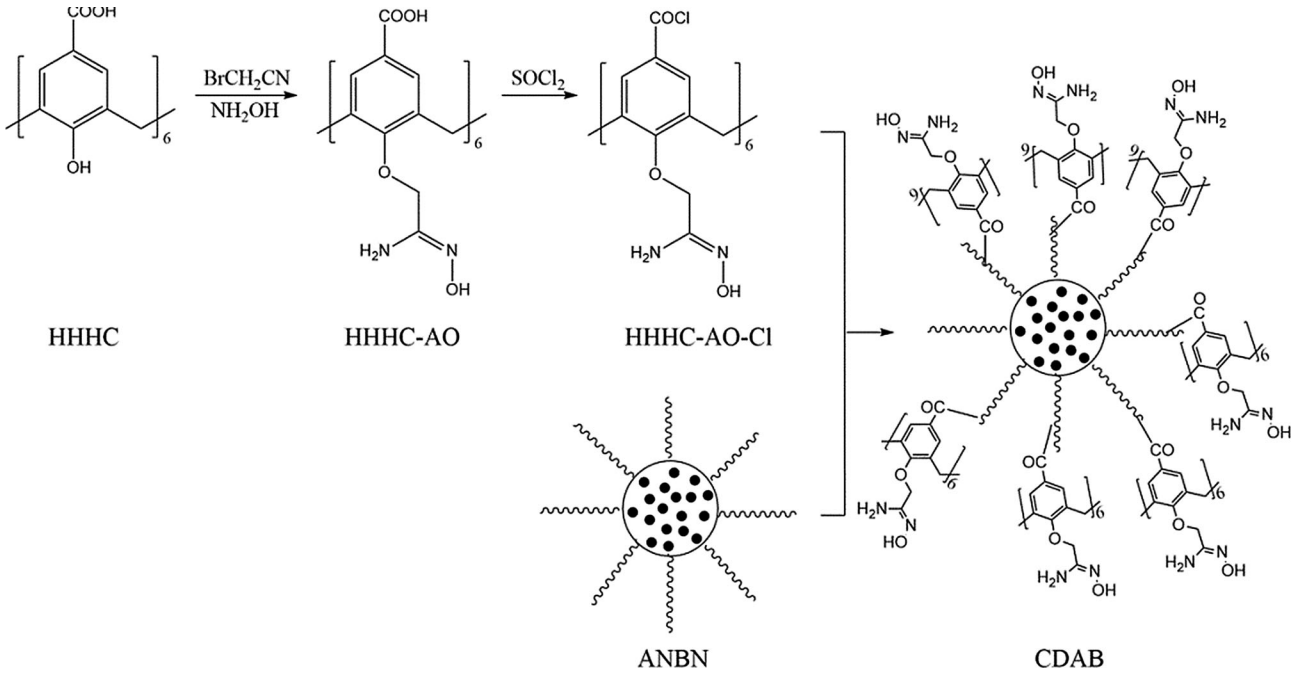

Scheme 1 Procedure for synthesizing the calix[6]arene derivative modified *Aspergillus niger*-Fe_3O_4 bio-nanocomposite (CDAB)

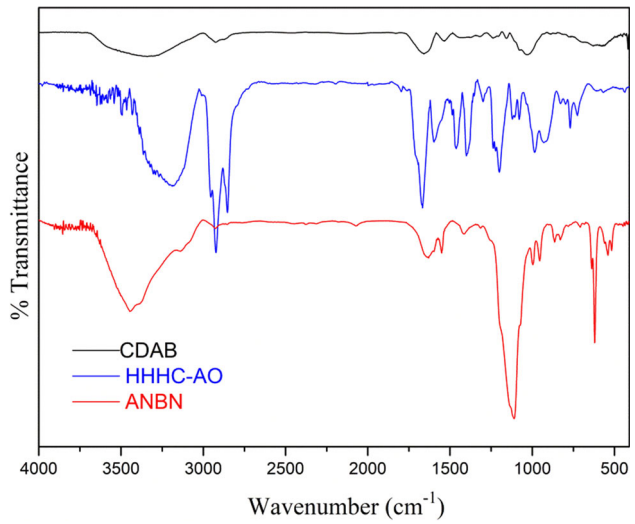

Fig. 2 FT-IR spectra of ANBN, HHHC-AO and CDAB

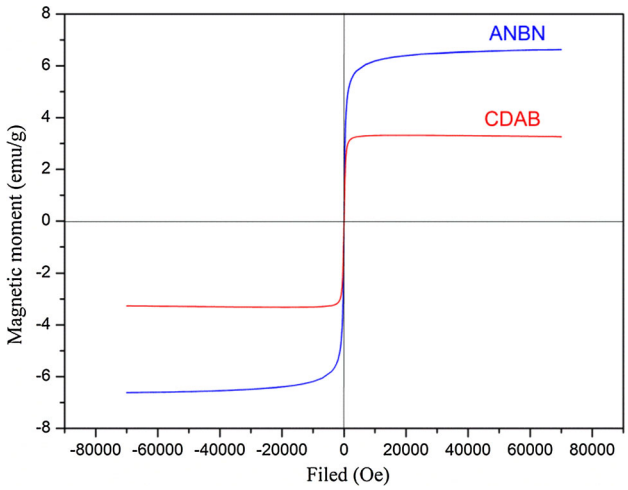

Fig. 4 Magnetization curves of ANBN and CDAB

CDAB (3.32 emu/g), which may be due to the HHHC-AO modification. There were no hysteresis loops and the remanence was negligible, which indicated that CDAB was still superparamagnetic.

The EDX spectra of CDAB and CDAB-U (uranium-loaded CDAB after adsorption) were shown in Fig. 5. Obviously, the presence of U elements in the CDAB material after adsorption of uranium (CDAB-U), indicating that uranium existed in the CDAB-U sample after adsorption. As shown in Fig. 6, a strong double U4f peak appeared in the XPS spectrum of CDAB-U, and the corresponding high-resolution $U4f_{5/2}$ and $U4f_{7/2}$ peaks at 392.48 and 381.68 eV, respectively, which further indicated that uranium(VI) existed in the CDAB-U sample after adsorption.

Effect of pH on uranium adsorption

Due to the significant impact on the adsorption property of adsorbent, the effect of pH on uranium adsorption by CDAB was firstly tested at different pH values ranging from 3 to 8. The result as shown in Fig. 7, the maximum removal efficiency of U(VI) from solution was obtained at pH 7. Therefore, as the optimum pH value, pH 7 was selected for the further adsorption experiments.

Effect of adsorbent dose on uranium adsorption

The effect of adsorbent dose on uranium adsorption by CDAB was investigated by changing the adsorbent dose from 5 mg to 50 mg. The results were shown in Fig. 8. It was clearly observed that the removal efficiency was increased with the increasing of adsorbent dose. Nevertheless, the adsorption capacity of uranium(VI) was decreased with the increasing of adsorbent dose. It was noted that the removal efficiency of uranium(VI) by CDAB increased slowly when the amount of adsorbent dose was greater than 30 mg. Therefore, 30 mg was selected as the appropriate adsorbent dose for the following adsorption experiments.

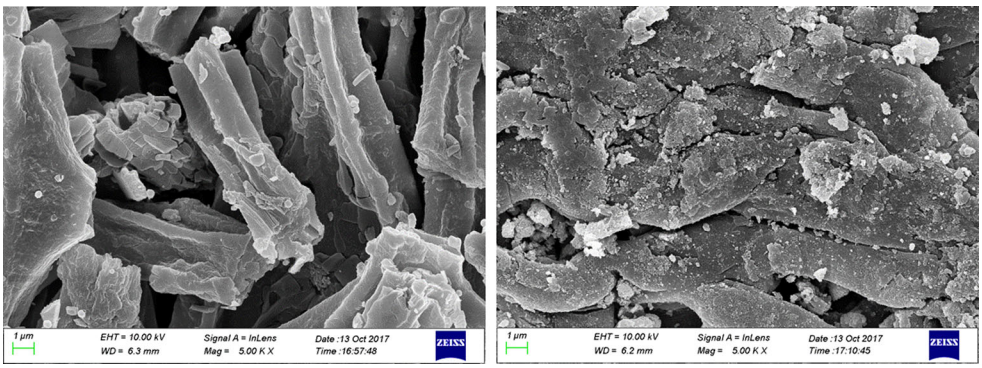

Fig. 3 SEM images of ANBN (left) and CDAB (right)

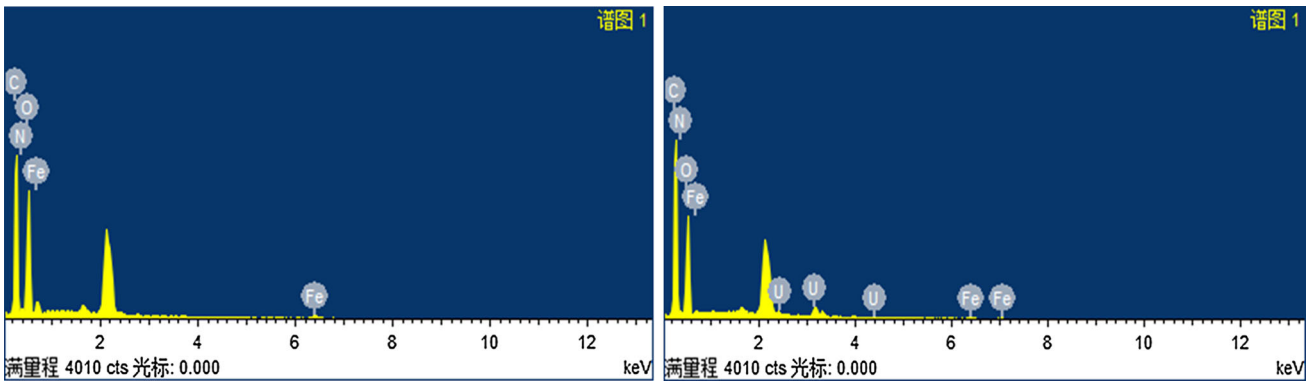

Fig. 5 EDX spectra of CDAB (left) and CDAB-U (right)

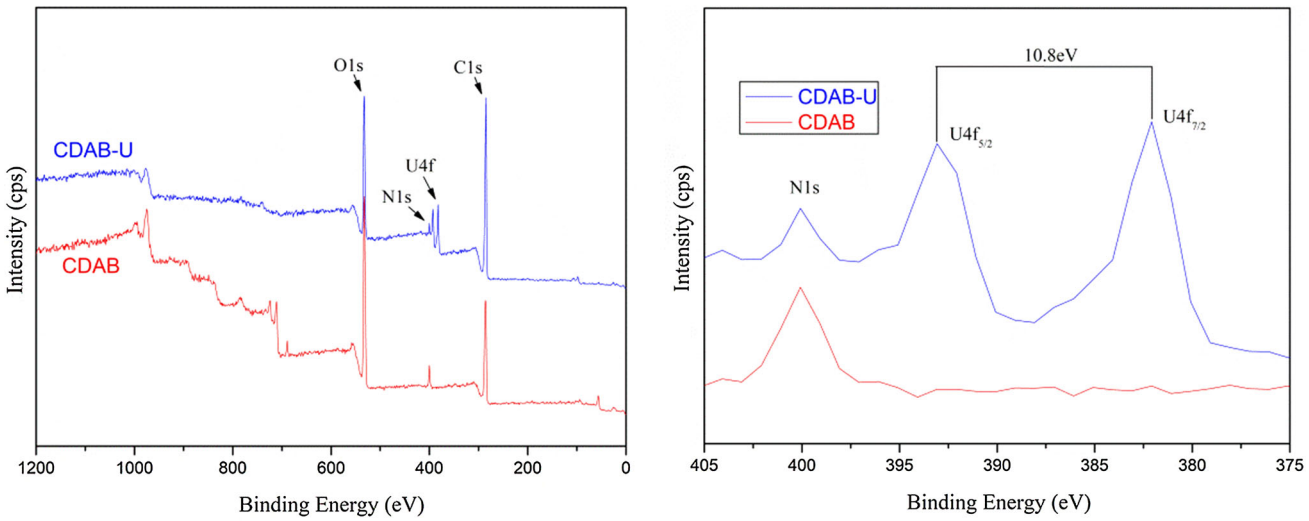

Fig. 6 XPS spectra of CDAB and CDAB-U

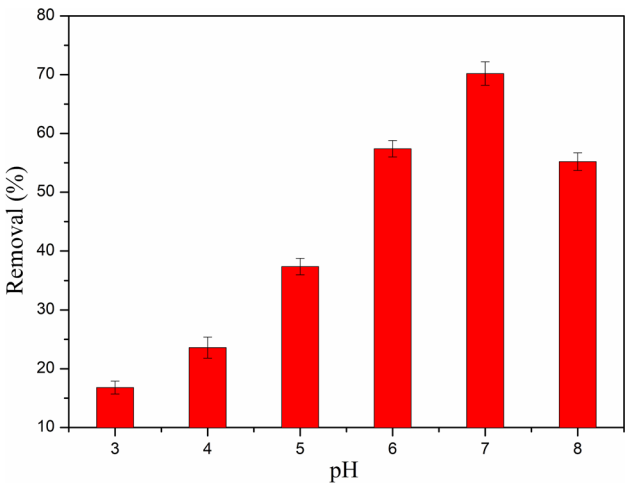

Fig. 7 Effect of pH on the U(VI) adsorption by CDAB (m = 15 mg, V = 100 mL, C_o = 10 mg/L, T = 298.15 K, t = 20 h)

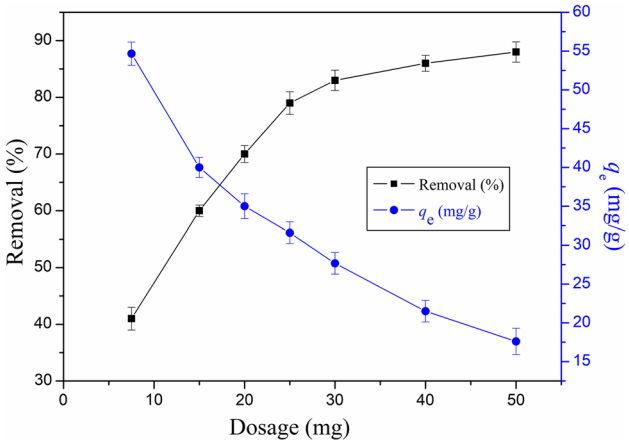

Fig. 8 Effect of adsorbent dose on the U(VI) adsorption by CDAB (pH 7, V = 100 mL, C_o = 10 mg/L, T = 298.15 K, t = 20 h)

Effect of contact time on uranium adsorption

Figure 9 showed the change of removal efficiency with contact time. In the first 3 h, the removal efficiency of uranium(VI) by CDAB was increased quickly, and reached equilibrium (83.6%) after 8 h. Thus, 8 h was selected as the contact time for the following adsorption experiments.

Effect of initial uranium concentrations on uranium adsorption

The effect of initial uranium concentrations on the U(VI) adsorption of CDAB was investigated by changing the concentrations from 10 to 100 mg/L. As shown in Fig. 10, it was clearly observed that the adsorption capacity of uranium was increased with the increasing initial uranium concentrations.

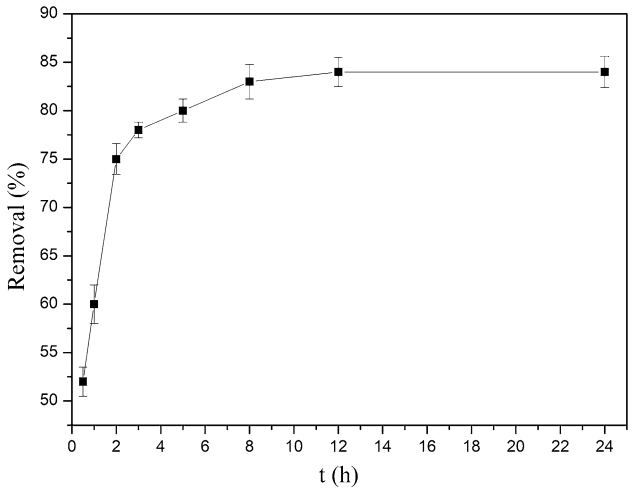

Fig. 9 Effect of contact time on the U(VI) adsorption by CDAB ($m = 30$ mg, pH 7, $V = 100$ mL, $C_o = 10$ mg/L, $T = 298.15$ K)

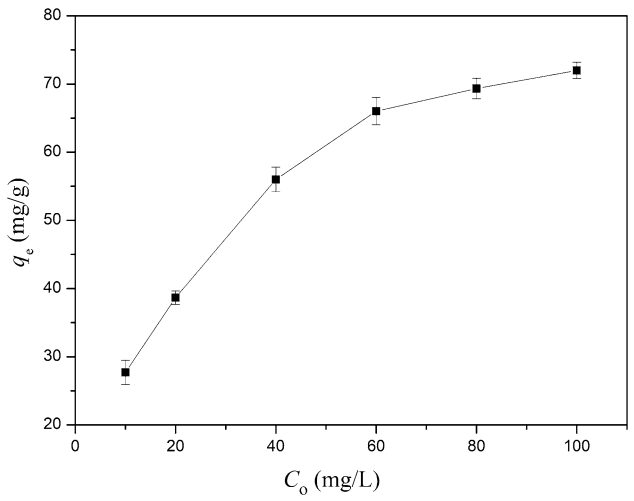

Fig. 10 Effect of initial uranium concentrations on the U(VI) adsorption by CDAB ($m = 30$ mg, pH 7, $V = 100$ mL, $T = 298.15$ K, $t = 8$ h)

Effect of temperature on uranium adsorption

The effect of temperature on the U(VI) adsorption of CDAB was investigated for temperature ranging from 298.15 to 318.15 K. The results showed that the adsorption capacity of uranium(VI) was increased with the increasing temperature as shown in Fig. 11. It may be due to the velocity of molecular movement was increased with the increasing temperature.

Effect of coexisting ions on uranium adsorption

The effect of coexisting metal ions, including Ca(II), Mn(II), Mg(II), Cd(II) and Zn(II), on the U(VI) adsorption of CDAB was investigated. The results were shown in Fig. 12 and listed in Table 1. Obviously, the q_e and K_d of CDAB for uranium(VI) were remarkably larger than other coexisting ions, which indicated that the bioadsorbent possessed a considerable selectivity for U(VI).

Adsorption kinetics

The adsorption kinetics often used to study the kinetic mechanism of the adsorption process. The adsorption experimental data were simulated with the pseudo-first-order and pseudo-second-order models.

The pseudo-first-order equation is as follows:

$$\ln(q_e - q_t) = \ln q_e - k_1 t. \quad (4)$$

The pseudo-second-order equation is as follows:

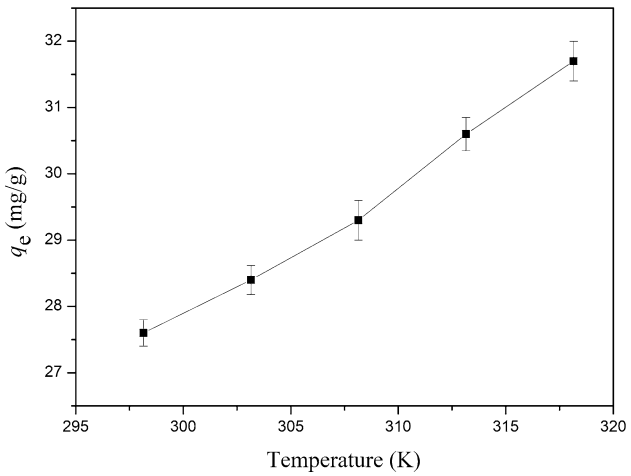

Fig. 11 Effect of temperature on the U(VI) adsorption by CDAB ($m = 30$ mg, pH 7, $V = 100$ mL, $C_o = 10$ mg/L, $t = 8$ h)

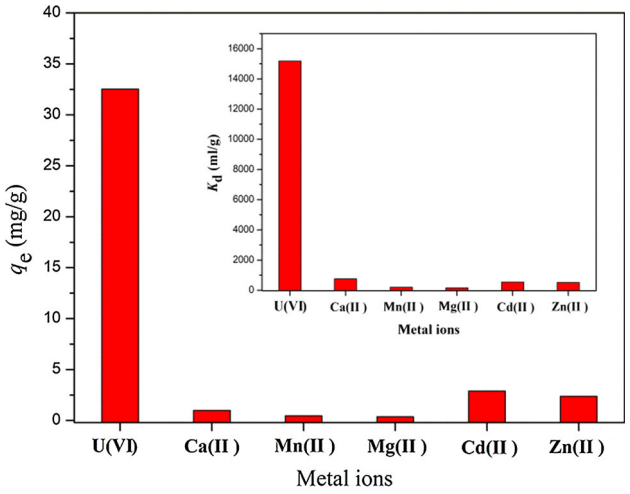

Fig. 12 Effect of coexisting ions on the U(VI) adsorption by CDAB ($m = 30$ mg, pH 7, $V = 100$ mL, $T = 298.15$ K, $t = 20$ h, $C_o \approx 0.05$ mmol/L for all metal ions)

Table 1 Adsorption capacity (q_e) and distribution coefficients (K_d) of CDAB

Ions	q_e (mg/g)	K_d (mL/g)
U(VI)	32.53	15,185.01
Ca(II)	1.02	755.72
Mn(II)	0.47	201.77
Mg(II)	0.37	148.12
Cd(II)	2.89	541.21
Zn(II)	2.37	517.41

$$\frac{t}{q_t} = \frac{1}{k_2 q_e^2} + \frac{1}{q_e} t, \tag{5}$$

where k_1 is the pseudo-first order adsorption rate constant, h^{-1}; k_2 is the second order adsorption rate constant, $g \cdot mg^{-1}\ h^{-1}$; q_e and q_t are the equilibrium adsorption capacity and the adsorption capacity at time t, mg g^{-1}.

The results was listed in Table 2. It was clearly seen that the pseudo-second-order model more suitable for described the U(VI) adsorption process of CDAB, because of the correlation coefficient (R^2) value (0.999) for the pseudo-second-order model greater than the correlation coefficient value (0.869) for the pseudo-first-order models. This result proved the adsorption process of CDAB was the chemical adsorption [22].

Adsorption isotherm

The Langmuir and Freundlich isotherm models were used to simulate the adsorption experimental data at different initial uranium concentrations. These two adsorption isotherm were given below:

Langmuir model:

$$\frac{C_e}{q_e} = \frac{1}{q_m b_L} + \frac{1}{q_m} C_e \tag{6}$$

Freundlich model:

$$\ln q_e = \ln K_F + \frac{1}{n_F} \ln C_e \tag{7}$$

Where C_e is the equilibrium concentration of U(VI) (mg/L). q_e is the amount of U(VI) adsorbed at equilibrium (mg/g). q_m and b_L are Langmuir constants related to maximum adsorption capacity and adsorption energy, respectively. K_F and n_F are Freundlich constants related to adsorption capacity and adsorption intensity, respectively.

The results was listed in Table 3. It was clearly seen that the Langmuir model more suitable for described the U(VI) adsorption process of CDAB, because of the correlation coefficient (R^2) value (0.9952) for the Langmuir model greater than the correlation coefficient value (0.9859) for the Freundlich model. This illustrated the adsorption process of CDAB was mainly a monolayer process [23]. In addition, the maximum adsorption capacities (q_m) of CDAB were calculated to be 77.04 mg g^{-1} for uranium(VI).

Adsorption thermodynamics

The mechanism of adsorption process was explored by adsorption thermodynamics. The adsorption experimental data at different temperature were simulated with the Van't Hoff equation as following:

Table 2 Kinetic parameters of U(VI) adsorption on CDAB

C_0 (mg L^{-1})	Pseudo-first-order			pseudo-second-order			q_e [mg g^{-1} (exp)]
	k_1 (h^{-1})	q_e (mg g^{-1})	R_1^2	k_2	q_e (mg g^{-1})	R_2^2	
10	0.2348	7.7898	0.8699	0.11997	28.4333	0.999	27.6667

Table 3 Parameters of the Langmuir and Freundlich isotherms

T (K)	Langmuir equation			Freundlich equation		
	q_m (mg g^{-1})	b_L (L mg^{-1})	R^2	n_F	K_F	R^2
298.15	77.0416	0.1545	0.9952	3.7896	23.6288	0.9859

Table 4 Thermodynamic parameters for adsorption of U(VI) onto CDAB

ΔH^0 (kJ/mol)	ΔS^0 (J/mol K)	ΔG^0 (kJ/mol)				
		298.15 (K)	303.15 (K)	308.15 (K)	313.15 (K)	318.15 (K)
48.88	186.20	− 6.61	− 7.54	− 8.47	− 9.40	− 10.33

$$\ln K_d = \frac{\Delta S^0}{R} - \frac{\Delta H^0}{RT} \quad (8)$$

Where K_d is the distribution coefficient (mL/g), ΔS^0 is the standard entropy (J mol^{-1} K^{-1}), ΔH^0 is the standard enthalpy (kJ mol^{-1}), T is the reaction temperature (K), and R is the gas constant (8.314 J mol^{-1} K^{-1}).

The standard Gibbs free energy (ΔG^0) values were calculated as follow:

$$\Delta G^0 = \Delta H^0 - T\Delta S^0. \quad (9)$$

The calculated thermodynamic parameters were listed in Table 4. The value of ΔH^0 is 48.88 kJ/mol, which indicates that the adsorption process was endothermic, and the positive value of ΔS^0 (ΔS^0 = 186.20 J/mol K) reveals that the adsorption was spontaneous and the randomness increased during the adsorption process. The values of ΔG^0 was decreased with increasing temperature of solution from 298.15 to 318.15 K, which indicates the adsorption process of uranium(VI) by CDAB was spontaneous and high temperature conducive to the adsorption process.

Conclusions

In summary, a calix[6]arene derivative modified *Aspergillus niger*-Fe_3O_4 bio-nanocomposite (CDAB) was successfully synthesized and used for removal of uranium (VI) from aqueous solutions. The adsorption experiment results showed that the adsorption efficiency of CDAB towards U(VI) could reach at 83.6% and had a considerable selectivity. The results of adsorption kinetic and isotherm indicate that the adsorption process were in accordance with pseudo-second order kinetic model and Langmuir adsorption isotherm model, which indicated that the adsorption process of CDAB was the chemical adsorption and mainly a monolayer process, respectively. In addition, based on the values of thermodynamic parameters, it could be found that the adsorption process was endothermic and spontaneous.

Acknowledgements This research was supported by the National Natural Science Foundation of China (11405081 and 51704170), the Natural Science Foundation of Hunan Province (2017JJ3276), the Department of Education of Hunan Province (17B226 and 15C1179), the Hunan Provincial Postgraduate Research and Innovation Project (CX2017B560).

References

1. Gralla F, Abson DJ, Møller AP, Lang DJ, Wehrden HV (2017) Energy transitions and national development indicators: a global review of nuclear energy production. Renew Sustain Energy Rev 70:1251–1265
2. Shu Y, Liu Z-M, Lin X-J, Wang R-Z (2016) A review of the development of nuclear waste treatment for China's Nuclear Power Industry. Adv Eng Res 94:322–326
3. Wang JQ, Li X, Li SP, Zhong H (2011) Studies on preparation of methotrexatum/layered double hydroxides compounds by coprecipitation method in ethanol-water medium. Acta Chim Sin 69:137–144
4. Liu Q, Zhu J, Tan L, Jing X, Liu J, Song D, Zhang H, Li R, Emelchenko G, Wang J (2016) Polypyrrole/cobalt ferrite/multi-walled carbon nanotubes as an adsorbent for removing uranium ions from aqueous solutions. Dalton Trans 45:9166–9173
5. Gorden AEV, Xu J, Raymond KN (2003) Rational design of sequestering agents for plutonium and other actinides. Chem Rev 103:4207–4282
6. Sather AC, Berryman OB, Rebek J (2010) Selective recognition and extraction of the uranyl ion. J Am Chem Soc 132:13572–13574
7. Helal AS, Mazario E, Mayoral A, Decorse P, Losno R, Lion C, Ammar S, Hémadi M (2018) Highly efficient and selective extraction of uranium from aqueous solution by a magnetic device: succinyl-β-cyclodextrin-APTES@maghemite nanoparticles. Environ Sci. https://doi.org/10.1039/c7en00902j
8. Ding DX, Tan X, Hu N, Li GY, Wang YD, Tan Y (2012) Removal and recovery of uranium(VI) from aqueous solutions by immobilized aspergillus niger powder beads. Bioprocess Biosyst Eng 35(9):1567–1576
9. Chen Z, Liang Y, Jia DS, Chen WY, Cui ZM, Wang XK (2017) Layered silicate RUB-15 for efficient removal of UO_2^{2+} and heavy metal ions by ion-exchange. Environ Sci Nano 4:1851–1858
10. Zarrougui R, Mdimagh R, Raouafi N (2018) Highly efficient extraction and selective separation of uranium(VI) from transition metals using new class of undiluted ionic liquids based on H-phosphonate anions. J Hazard Mater 342(15):464–476
11. Li L, Hu N, Ding D, Xin X, Wang YD, Xue JH (2015) Adsorption and recovery of U(VI) from low concentration uranium solution by amidoxime modified *Aspergillus niger*. RSC Adv 5(81):65827–65839
12. Bayramoglu G, Akbulut A, Arica MY (2015) Study of polyethyleneimine- and amidoxime-functionalized hybrid biomass of *Spirulina (Arthrospira) platensis* for adsorption of uranium(VI) ion. Environ Sci Pollut Res 22(22):17998–18010
13. Bayramoglu G, Arica MY (2016) Amidoxime functionalized *Trametes trogii* pellets for removal of uranium(VI) from aqueous medium. J Radioanal Nucl Chem 307(1):373–384
14. Bayramoglu G, Arica MY (2015) MCM-41 silica particles grafted with polyacrylonitrile: modification into amidoxime and carboxyl groups for enhanced uranium removal from aqueous medium. Microporous Mesoporous Mater 226:117–124
15. Arica MY, Bayramoglu G (2016) Polyaniline coated magnetic carboxymethylcellulose beads for selective removal of uranium

ions from aqueous solution. J Radioanal Nucl Chem 310(2):711–724
16. Bayramoglu G, Arica MY (2017) Polyethylenimine and tris(2-aminoethyl)amine modified p(GA–EGMA) microbeads for sorption of uranium ions: equilibrium, kinetic and thermodynamic studies. J Radioanal Nucl Chem 312(2):293–303
17. Bayramoglu G, Akbulut A, Acıkgoz-Erkaya I, Arica MY (2017) Uranium sorption by native and nitrilotriacetate-modified *Bangia atropurpurea* biomass: kinetics and thermodynamics. J Appl Phycol. https://doi.org/10.1007/s10811-017-1238-8
18. Li L, Xu MZ, Chubik M, Chubik M, Gromov A, Wei GD, Han W (2015) Entrapment of radioactive uranium from wastewater by using fungus-Fe_3O_4 bio-nanocomposites. RSC Adv 5(52):41611–41616
19. Ding CC, Cheng WC, Sun YB, Wang XK (2015) Novel fungus-Fe_3O_4 bio-nanocomposites as high performance adsorbents for the removal of radionuclides. J Hazard Mater 295:127–137
20. Lu X, He SN, Zhang DX, Reda AT, Liu C, Feng J, Yang Z (2016) Synthesis and characterization of amidoxime modified calix[8]-arene for adsorption of U(VI) in low concentration uranium solution. RSC Adv 6:101087–101097
21. Trivedi UV, Menon SK, Agrawal YK (2002) Polymer supported calix[6]arene hydroxamic acid, a novel chelating resin. React Funct Polym 50:205–216
22. Tan X, Ren X, Li J, Wang X (2013) Theoretical investigation of uranyl ion adsorption on hydroxylated γ-Al_2O_3 surfaces. RSC Adv 3:19551–19559
23. Anirudhan TS, Bringle CD, Rijith S (2012) Removal of uranium(VI) from aqueous solutions and nuclear industry effluents using humic acid-immobilized zirconium-pillared clay. J Environ Radioact 101:267–276